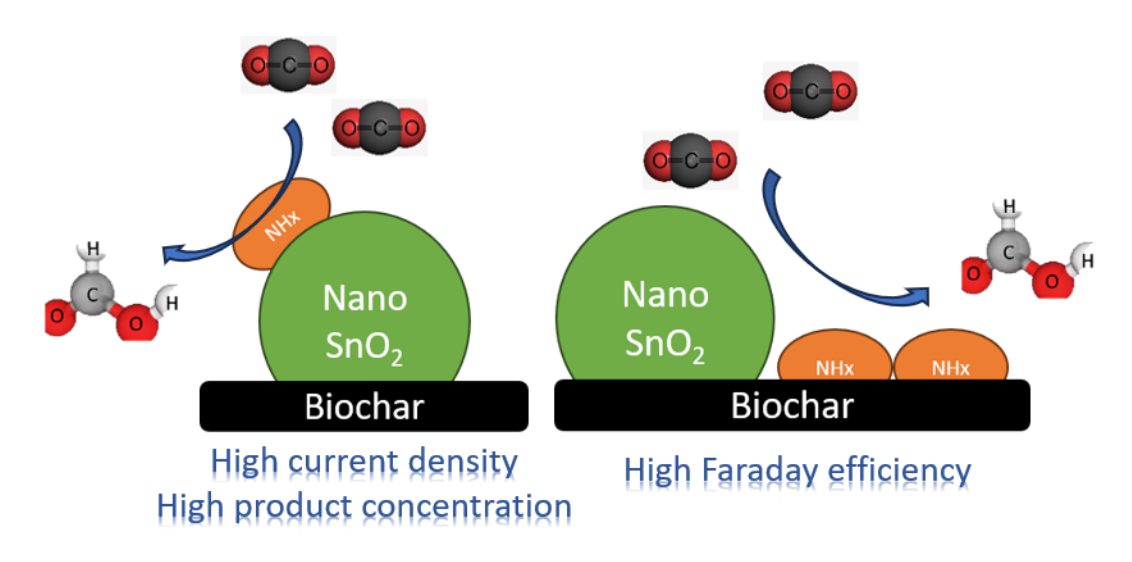
The Influence of Amino Anchoring Position on SnO₂/Biochar for Electroreduction of CO₂ to HCOOH

Mingxue Su a,b,* and Ning Li a,b

*Corresponding author:smx123@mail.ustc.edu.cn

DOI: 10.15376/biores.19.4.9049-9059

GRAPHICAL ABSTRACT



The Influence of Amino Anchoring Position on SnO₂/Biochar for Electroreduction of CO₂ to HCOOH

Mingxue Su a,b,* and Ning Li a,b

Biochar derived from biomass resources as a carrier to load SnO₂ for electroreduction of CO2 not only can benefit carbon emissions, but it also can achieve waste utilization. However, the weak CO2 mass transfer and conductivity ability of SnO₂/biochar limits its applications to such eCO₂RR processes. This study focused on modifying SnO₂/biochar with amino groups and investigated the effects of positioning of amino groups on the catalyst's physicochemical properties and electrocatalytic behaviors. Elemental analysis revealed that anchoring amino groups on biochar (SnO₂/C-NHx) is advantageous for increasing amounts of amino groups attached, thereby enhancing biochar adsorption energy and subsequently increasing the loading of Sn. The CO2 adsorption curve indicated that amino groups anchored on biochar facilitate CO₂ adsorption due to high specific surface area of biochar. X-ray photoelectron spectroscopy showed that amino groups anchored on SnO2 (NHx-SnO2/C) resulted in highly electron-rich centers on Sn, which promoted electron transfer between the catalyst and CO2. Electrochemical tests demonstrated the improved performance of amino-modified SnO₂/biochar. SnO₂/C-NHx exhibited enhanced Faraday efficiency, whereas NHx-SnO₂/C showed higher current density. The disparity in electrochemical performance can be mainly attributed to the different selectivity towards rate-controlling steps of electron transfer and mass transfer induced by the various positions of amino groups anchoring.

DOI: 10.15376/biores.19.4.9049-9059

Keywords: Amino; Anchoring position; Tin oxide; Biochar; CO₂ electroreduction

Contact information: a: Hefei Cement Research and Design Institute Corporation Ltd, Hefei, 230022, Anhui, China; b: Anhui Key Laboratory of Green and Low-carbon Technology in Cement Manufacturing, Hefei, 230022, Anhui, China; *Corresponding author: smx123@mail.ustc.edu.cn

INTRODUCTION

Compared to photo and thermal reduction methods, electrochemical CO₂ reduction reaction (eCO₂RR) is a more economical and environmentally friendly approach for CO₂ conversion to organic chemicals (Han et al. 2019). Among the array of CO₂ electroreduction products, formic acid (HCOOH) has garnered attention due to its versatility as a raw material for various chemicals and its role as a safe hydrogen storage carrier (Wang et al. 2022). Notably, HCOOH surpasses competitors such as carbon monoxide (CO) and methanol (CH₃OH) in terms of electrochemical production cost (Jouny et al. 2018).

Numerous metallic elements, particularly their oxides, can serve as catalysts for CO₂ electroreduction to HCOOH. SnO₂ has garnered attention due to its affordability, nontoxicity, and high Faraday efficiency (FE) in HCOOH production (Kim et al. 2019), and it has been studied from various aspects such as particle size, morphology and content. Zhang

et al. (2014) reported the electrocatalytic reduction of CO₂ to HCOOH using carbon black loaded with small-sized nano SnO₂ (3 to 6 nm). The FE was 90%, but the current density was only 5 mA/cm². Liu et al. (2017) investigated the urchin-like nanostructured SnO₂ and the FE of 62% was achieved. Yu et al. (2017) found that low SnO2 content led to insufficient catalytic sites, and high SnO₂ content led to aggregation and blockage of catalytic sites, which are unfavorable for CO2 reduction. Nevertheless, studies have revealed that the FE_{HCOOH} of SnO₂ plateaus at 60 to 70% (Hu et al. 2018; Tay et al. 2021; Yuan et al. 2021; Yue et al. 2023). To enhance SnO2's electrocatalytic efficiency, researchers have explored the integration of carbon materials and amino functional groups (Lu et al. 2017; Meng et al. 2019a; Cheng et al. 2021; Zhang et al. 2021). Biochar, a carbon material obtained through pyrolysis of waste biomass, could act as the carrier and boost conductivity and specific surface area of catalyst, thereby facilitating contact with CO2 and charge transfer (Fu et al. 2023; Hu et al. 2024). Tan et al. (2023) studied coconut huskderived biochar for enhancing electrochemical conversion of CO₂, and 140 mA/cm² current density was achieved. Zhang et al. (2023) engineered the porosity of biochar to promote the electroreduction performance of single-atom Ni. Grafting amines onto catalysts is a strategy to further improve the electroreduction of catalysts because amino functional groups, serving as Lewis bases, can accelerate the adsorption and mass transfer of CO₂ on SnO₂ (Petrovic et al. 2021). Besides, the N atom in the amino group can also improve the chemical environment of SnO₂ (Lin et al. 2022). Optimizing the composition and structure of tin oxide, biochar, and amino groups is crucial for enhancing SnO2's electrocatalytic efficiency. Among these factors, the anchoring position of amino groups is a pressing concern. Various studies have shown that the role of surface modification functional groups varies with the anchoring position of the catalyst, especially for catalysts with complex structures (Sun et al. 2017; Meng et al. 2019b; Mulik et al. 2021). For instance, Dou et al. (2022) demonstrated that Co-N₄ sites anchored on the edge of hierarchical porous structures exhibit higher selectivity in electroreduction of O₂ compared to those anchored on the basal plane. Given that SnO₂ with biochar forms a composite catalyst, both the biochar carrier and the SnO₂ active sites can anchor amino groups. The anchoring points of amino groups inevitably exert a significant impact on the physicochemical properties of the overall catalyst and the characteristics of CO₂ electroreduction. However, there is currently a lack of clear and systematic research on this aspect.

In this study, diethanolamine and rice husk serve as a representative amino functional group and a raw material for biochar, respectively. Biochar was prepared by pyrolysis and hydrothermal methods, and amino groups were anchored onto the biochar carrier and nano tin oxide active sites. The impact of various amino group anchoring points on the physicochemical properties, CO₂ adsorption, and electroactivity of tin oxide was investigated.

EXPERIMENTAL

Materials

Diethanolamine (AR, DEA), dicyclohexylcarbodiimide (AR, DCC), dimethyl formamide (AR, DMF), ethanol (AR), tin (II) chloride (AR, SnCl₂), potassium bicarbonate (AR, KHCO₃), sulfuric acid (AR, 98 wt%, H₂SO₄), ammonium hydroxide solution (AR, NH₄OH), and nitric acid (AR, 69.5 wt%, HNO₃) were procured from Sinopharm Chemical Reagent Co., Ltd. (Shanghai, China). Rice husk was sourced from local farmland (Hefei,

China). Carbon paper sheets were supplied by Toray (Japan). Nafion solution (5 wt%) and Nafion 117 membranes were obtained from DuPont (USA). All reagents and materials were used directly.

Catalyst Preparation

Biochar was produced by pyrolysis of rice husk at 550 °C in a nitrogen atmosphere and was labeled as C. Amination of biochar was conducted following procedures outlined in prior literature (Cheng et al. 2017). Initially, biochar underwent oxidation using a mixture of concentrated H₂SO₄ and HNO₃. Subsequently, a specific amount of DEA was fully dispersed in DMF after ultrasonic treatment, followed by the addition of DCC and the oxidized biochar. The mixture was stirred for 24 h at 135 °C, and the resulting solution was filtered. The filtered mixtures were then washed with ethanol and dried overnight at 90 °C. The resulting product was designated as C-NHx.

A series of SnO₂-supported biochar catalysts modified by amino groups were synthesized using a straightforward hydrothermal method (Jiang et al. 2005). Typically, 1 g of SnCl₂ was dissolved in 80 mL mixture of ethanol and DIW, and then 200 mg of C was added to the solution. After stirring, NH₄OH was added to adjust pH, and then the mixture was refluxed at 100 °C, followed by centrifugation, washing with ethanol, and drying. The resulting product was labeled as SnO₂/C. Alternatively, by substituting C with C-NHx, the resulting product was designated as SnO₂/C-NHx, indicating that the amino groups are anchored on the biochar carrier. To anchor amino groups onto nano SnO2, 0.5 g of DEA was added before the reflux process, and the obtained product was labeled as NHx-SnO₂/C, indicating that the amino groups are located on the nano SnO₂. The material obtained by impregnating SnO₂/C into DEA-ethanol solution was named NHx-loaded SnO₂/C.

Identification of Catalysts

Powder X-ray diffraction (XRD) patterns were obtained using a Smart Lab X-ray diffractometer (XRD, Japan) equipped with a Cu-Ka source. Fourier transform infrared spectroscopy (FTIR) analysis of the functional chemicals was performed using a ThermoFisher Nicolet IS20 instrument (USA) with KBr disks. X-ray photoelectron spectra (XPS) were collected using a Thermo ESCALAB 250 instrument (USA) with an Al K α Xray source. CO₂ and N₂ adsorption-desorption isotherms were measured using a ChemStar TPx chemisorption analyzer (Quantachrome Instrument, USA). The content of Sn was analyzed using inductively coupled plasma mass spectrometry (ICP-MS, Thermo Fisher iCAP RQ, USA), while the nitrogen content was determined using an elemental analyzer (Vario EL cube, Germany). Transmission electron microscopy (TEM) on a JEM-2010 (HR) was operated at an accelerating voltage of 300 kV.

Electrochemical Experiments

Initially, 10 mg of catalyst was dispersed in 1 mL of ethanol containing 100 µL of Nafion[™] solution *via* ultrasonic dispersion. The resulting mixture was then sprayed onto carbon paper (1 cm²) repeatedly until the desired loading amount of 1 mg was achieved. The prepared working electrode and a standard electrode (Ag/AgCl) were placed in the cathodic chamber, with a counter electrode (Pt sheet) in the anodic chamber. The cathodic and anodic chambers were separated by a Nafion 117 membrane, and a 0.5 M KHCO₃ solution was used as the electrolyte. High-purity CO₂ was introduced for at least 30 min before performing linear sweep voltammetry (LSV) and chronoamperometry (i-t) studies. Liquid products were analyzed using ion chromatography (IC, Metrohm Eco, Switzerland),

while gaseous products were analyzed using gas chromatography (GC, Thermo Trace 1310, USA) equipped with a flame ionization detector (FID) and a thermal conductivity detector (TCD). The FE for formic acid (FE_{HCOOH}) was calculated by Eq. 1,

$$FE = \frac{2 \times n \times F}{Q} \times 100\% \tag{1}$$

where n, F, and Q represent the amount of HCOOH per mole, Faraday's constant (96485 C/mol), and charge (C), respectively.

The FE for CO and H₂ were calculated using Eq. 2,

$$FE = \frac{10^{-3} \times 2 \times v\% FG}{60RTL} \times 100\% \tag{2}$$

where v%, G, R, T, and I represent the concentration of CO or H₂, CO₂ flow rate (10 mL/min), gas constant (8.314 J/mol/K), temperature (298 K), and constant current (A), respectively.

RESULTS AND DISCUSSION

XRD spectra were utilized to analyze the crystal phase of each catalyst. As depicted in Fig. 1, all catalysts exhibited similar diffraction peaks at $2\theta = 27^{\circ}$ and 52° , corresponding to the (110) and (211) planes in the crystalline phase of SnO₂, respectively. Additionally, weak diffraction peaks at $2\theta = 43^{\circ}$ were attributed to the characteristic peaks of carbon (Yua *et al.* 2017). This suggests that SnO₂ is loaded onto biochar, and the different anchoring points of amino groups do not affect the crystal phase of SnO₂ active sites.

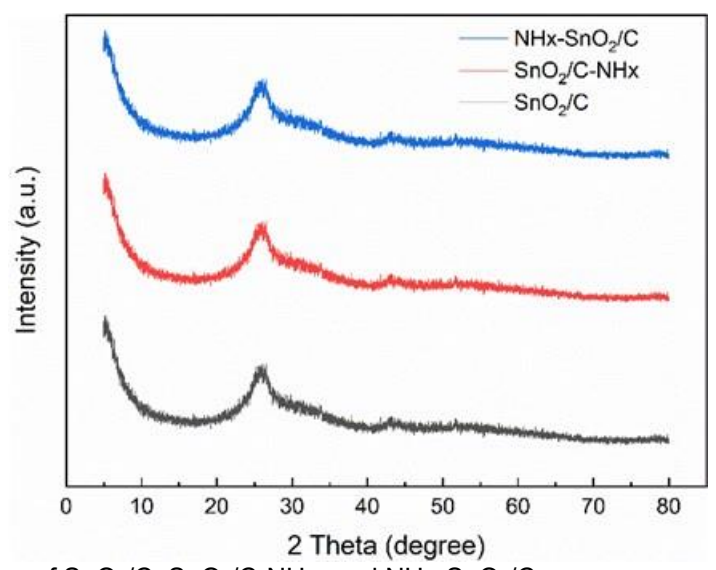


Fig. 1. XRD patterns of SnO₂/C, SnO₂/C-NHx, and NHx-SnO₂/C

The FTIR spectrum in Fig. 2 reveals the presence of functional groups in all catalysts. The characteristic peak observed in the range of 1500 to 1700 cm⁻¹ was attributed to the bending vibration characteristic peaks of -NH, indicating the presence of amino functional groups anchored on all catalysts.

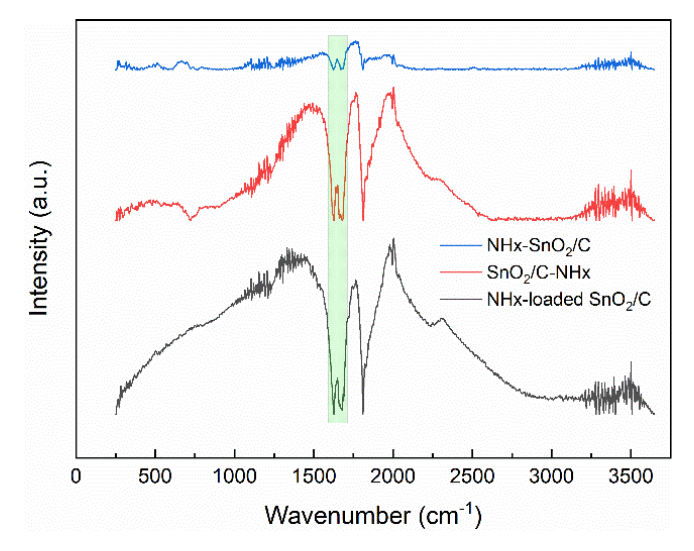


Fig. 2. FTIR spectra of SnO₂/C-NHx, NHx-SnO₂/C, and NHx-loaded SnO₂/C

Table 1 summarizes the textural properties and elemental content of all catalysts. The Sn and N contents of SnO₂/C-NHx were found to be 27.9% and 0.99%, respectively, which were higher than those of SnO₂/C and NHx-SnO₂/C. Based on the catalyst preparation process, it can be inferred that biochar with a high specific surface area (S_{BET}) can anchor more amino functional groups compared to nano SnO2, and amino groups anchored on biochar also can enhance the adsorption energy of biochar, thereby increasing the loading amount of SnO₂. The specific surface area (S_{BET}) of SnO₂/C was 63.1 m²/g, which was lower than 99.2 m²/g of NHx-SnO₂/C and 67.5 m²/g of SnO₂/C-NHx. This phenomenon indicated that amino groups are beneficial for the dispersion of tin oxide on biochar, as the Sn content of SnO₂/C was significantly lower than NHx-SnO₂/C and SnO₂/C-NHx and theoretically S_{BET} of SnO₂/C should be higher. Simultaneously, it has been reported that amine substances can reduce the aggregation of metallic oxides during the formation process (Cheng et al. 2021), which also supported this phenomenon and inference. Furthermore, the order of decrease of SBET was NHx-SnO₂/C < SnO₂/C-NHx, meaning that amino groups anchored on SnO₂ were more effective in delaying the aggregation of SnO₂ compared to amino groups anchored on biochar.

Table 1. Textural Properties and Content of N and Sn for SnO₂/C, SnO₂/C-NHx, and NHx-SnO₂/C

Samples	^а Ѕвет (m²/g)	Content of N (%)	Content of Sn (%)
С	263.1	0.03	1
SnO ₂ /C	63.1	0.03	24.8
NHx-SnO ₂ /C	99.2	0.62	25.6
SnO ₂ /C-NHx	67.5	0.99	27.9
NHx-loaded SnO ₂ /C	61.6	0.65	24.3

^aDetermined by N₂ adsorption-desorption isotherms at 77 K

The TEM images also clearly revealed the influence of different amino anchor sites on the size of tin oxide. As shown in Fig. 3, tin oxide aggregates to particles of about 20 nm, but the agglomeration phenomenon of NHx-SnO₂/C was significantly lighter than that of SnO₂/C-NHx. This result also supported the inference that amino groups anchored on SnO₂ are more effective in delaying the aggregation.

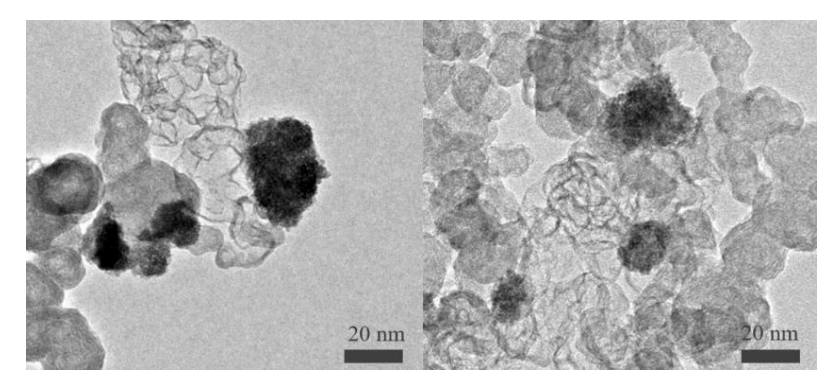


Fig. 3. TEM images of SnO₂/C-NHx (left) and NHx-SnO₂/C (right)

All investigated catalysts were comprehensively analyzed for their compositions and chemical states using profiles obtained from XPS. As depicted in Fig. 4, compared to SnO₂/C and SnO₂/C-NHx, the O 1s peak of NHx-SnO₂/C shifted to a higher binding energy, suggesting the presence of more oxygen deficit sites. Additionally, the N 1s and Sn 3d signals of NHx-SnO₂/C shifted to lower binding energies, indicating a possible transfer of electrons from N to Sn. Consequently, the highly electron-rich centers of Sn species in NHx-SnO₂/C facilitate CO₂ activation. Moreover, the generated electrostatic field accelerates charge transfer (Lu *et al.* 2017). These findings suggest that the amino group anchored on nano SnO₂ had a more pronounced effect on the chemical state of SnO₂ compared to the amino group anchored on biochar.

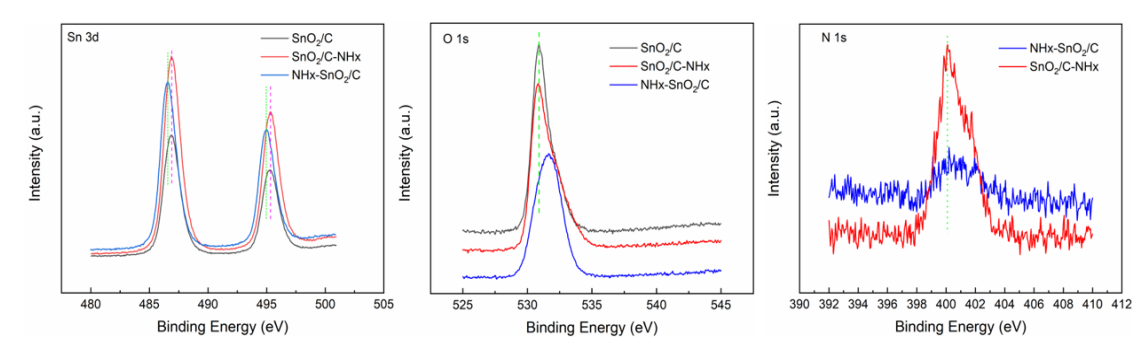


Fig. 4. XPS spectra of Sn 3d (left), O 1s (middle) and N 1s (right) for SnO₂/C, SnO₂/C-NHx, and NHx-SnO₂/C

The CO₂ adsorption capacity of all catalysts was investigated using CO₂ isothermal adsorption curves. As depicted in Fig. 5, the highest CO₂ adsorption capacity was observed for SnO₂/C-NHx at 5.7 cm³/g. In contrast, NHx-SnO₂/C exhibited a CO₂ adsorption capacity of 2.2 cm³/g, which was slightly higher than 1.9 cm³/g observed for SnO₂/C. NHx-loaded SnO₂/C also demonstrated a CO₂ adsorption capacity of 4.5 cm³/g, despite having a similar N content to NHx-SnO₂/C. Furthermore, the S_{BET} of SnO₂/C was lower than that of NHx-SnO₂/C, theoretically leading to a higher CO₂ adsorption capacity for NHx-SnO₂/C. Therefore, it can be inferred that amino groups anchored on biochar were more conducive to CO₂ adsorption than those anchored on SnO₂. This may be attributed to the high S_{BET} of biochar, facilitating the interaction of amino groups anchored on biochar with CO₂.

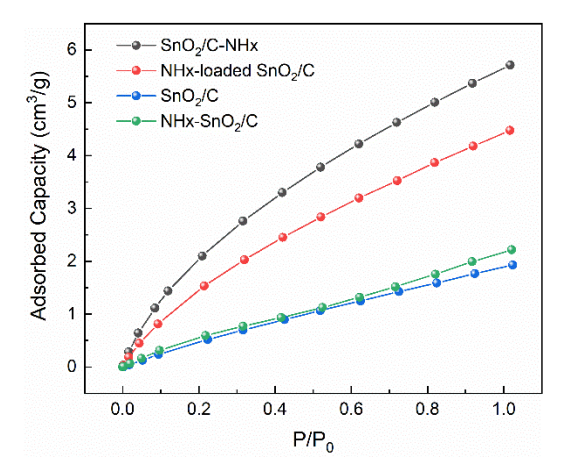


Fig. 5. CO₂ adsorption isotherms for SnO₂/C, SnO₂/C-NHx, NHx-loaded SnO₂/C, and NHx-SnO₂/C

A series of LSV and chronoamperometry (i-t) experiments were conducted to assess the electrochemical performances of all catalysts. As shown in Fig. 6(a), compared to the N₂-saturated solution, all catalysts exhibited increased current levels in the CO₂-saturated solution across the investigated potential range, indicating that eCO₂RR was favored over the hydrogen evolution reaction (HER). Tafel slopes evaluated from the LSV curves of all catalysts in the CO₂-saturated electrolyte are displayed in Fig. 6(c), representing the rate-controlling step of an initial single electron shift from the catalysts to CO₂ generally (Jeong *et al.* 2021).

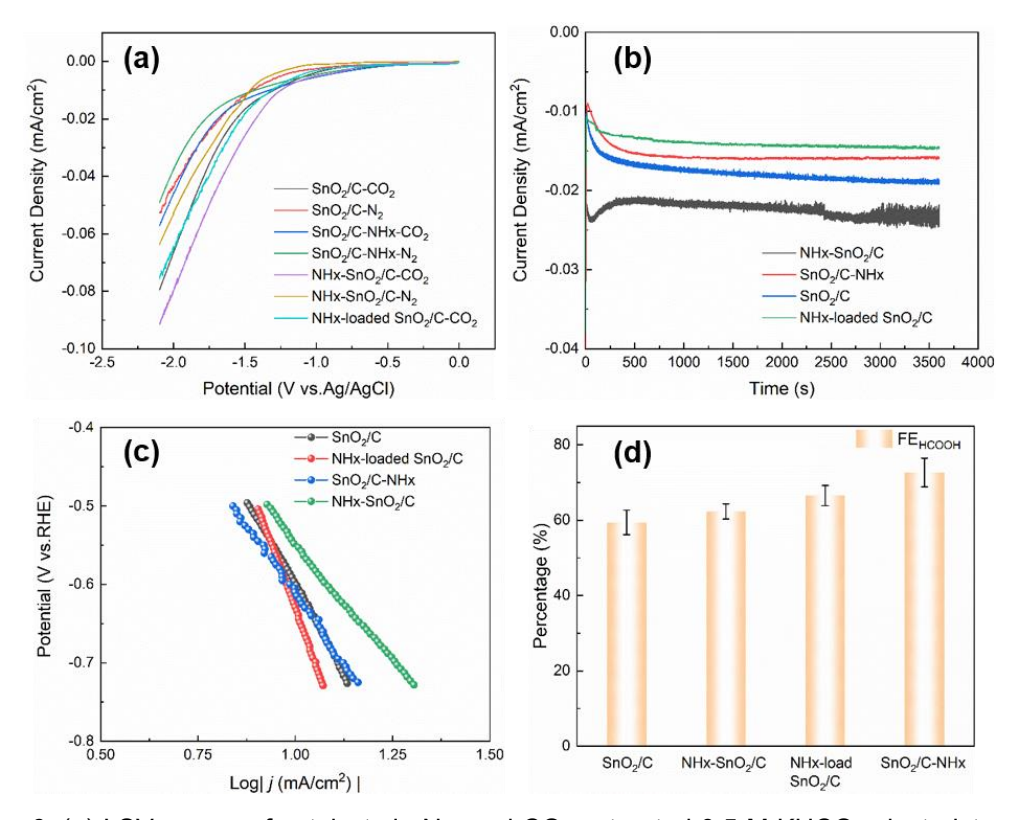


Fig. 6. (a) LSV curves of catalysts in N_2 - and CO_2 -saturated 0.5 M KHCO $_3$ electrolytes at a scan rate of 50 mV/s, (b) i-t curves of catalysts at the potential -1.5 V vs. Ag/AgCl, (c) Tafel slopes curves of catalysts and (d) FE of HCOOH at the potential -1.5 V vs. Ag/AgCl after 1 h of eCO $_2$ RR

I-t tests of various catalysts at -1.5 V (*vs.* Ag/AgCl) for 1 h were performed to determine the FE for formic acid (FE_{HCOOH}) and current density. The average current densities were approximately 22, 17, 15, and 12 mA/cm² for NHx-SnO₂/C, SnO₂/C, SnO₂/C, SnO₂/C, NHx, and NHx-loaded SnO₂/C, respectively. It was evident from the comparison that NHx-SnO₂/C could accelerate the electron transfer from Sn to CO₂, which was also corresponding to XPS analysis. This indicates that NHx-SnO₂/C exhibited superior electrochemical performance compared to other catalysts. However, the FE_{HCOOH} presented different results. As shown in Fig. 6(d), SnO₂/C-NHx exhibited an FE_{HCOOH} of 73.3%, higher than 67.4%, 64.1%, and 59.1% for NHx-loaded SnO₂/C, NHx-SnO₂/C, and SnO₂/C, respectively. These results indicate that the influence of amino anchoring position on current density and FE was significantly different. The amino group anchored on biochar was beneficial for improving FE, while the amino group anchored on SnO₂ was favorable for increasing current density.

To further elucidate this difference, Table 2 summarized the concentration of HCOOH over all of the catalysts. Although the current density of SnO₂/C-NHx was lower than SnO₂/C, CO₂ was still converted into more HCOOH by SnO₂/C-NHx. Actually, even in the CO₂-saturated solution, current density is still co-determined by proton and CO₂ reduction (Jeong et al. 2021). Therefore, the decrease in current density of SnO₂/C-NHx might have been due to the suppression of HER because of enhanced CO₂ adsorption capacity of SnO₂/C-NHx based on the CO₂ adsorption isotherm. More electricity was used to convert CO₂, and this resulted in the highest FE_{HCOOH} for SnO₂/C-NHx. Conversely, NHx-SnO₂/C exhibited a higher concentration of HCOOH (236 ppm vs. 184 ppm) and a larger current density (22 mA/cm² vs. 15 mA/cm²) due to improved electron transfer between CO₂ and highly electron-rich centers of Sn species caused by anchoring amino groups on SnO₂ based on XPS results. This indicated that NHx-SnO₂/C was superior in conductivity and electrochemical rate as confirmed by LSV, i-t, and Tafel slope tests. However, a high-speed conversion rate meant that CO₂ was consumed rapidly on the catalyst surface. Due to the poor CO2 adsorption capacity, NHx-SnO2/C could not fully contact with the CO₂ source during electroreduction. This resulted in ineffective inhibition of HER, which was reflected in decreased FEHCOOH compared to SnO₂/C-NHx. It is well known that the rate-determining steps of eCO₂RR are divided into electrochemical processes and mass transfer processes. Thereby, the amino group anchored on biochar exerted on CO₂ mass transfer process to achieve high FE_{HCOOH}, but the amino group anchored on SnO₂ acted on electrochemical processes for increasing current density and high HCOOH concentration.

Table 2. Concentration of HCOOH Catalyzed by All Catalysts

Catalysts	Concentration of HCOOH (ppm)	
SnO ₂ /C-NHx	184	
NHx-SnO ₂ /C	236	
NHx-loaded SnO ₂ /C	135	
SnO ₂ /C	168	

CONCLUSIONS

- 1. Amino functional groups can enhance the activity of SnO₂/biochar catalyst for the electroreduction of CO₂. However, the influence of amino anchoring position on the reaction process is significantly different.
- 2. The amino group anchored on biochar is advantageous for the adsorption of CO₂ due to the high specific surface area of biochar, improving the FE of HCOOH through enhanced mass transfer processes. Conversely, the amino group anchored on SnO₂ is favorable for the charge transfer between CO₂ and highly electron-rich centers of Sn active site caused by transfer of electrons from N to Sn, increasing the current density of eCO₂RR *via* boosting electron transfer processes.
- 3. From the perspective of product concentration, anchoring amino groups on nano tin oxide (NHx-SnO₂/C) is a more suitable modification strategy.

ACKNOWLEDGMENTS

The Chinese Ministry of Sciences and Technology of the PRC provided a grant for this research under its National Key Development and Research Program (No. 2020YFC1908704).

REFERENCES CITED

- Cheng, Y. L., Xia, B. B., Fang, C. Q., and Yang, L. (2017). "Structure, mechanical and thermal properties of BMI/E-44/CNTs ternary composites *via* amination method," *J Mater. Sci. Technol.* 33, 1187-1194. DOI: 10.1016/j.jmst.2017.04.013
- Cheng, Y. Y., Hou, J., and Kang, P. (2021). "Integrated capture and electroreduction of flue gas CO₂ to formate using amine functionalized SnOx nanoparticles," *ACS Energy Lett.* 6, 3352-3358. DOI: 10.1021/acsenergylett.1c01553
- Fu, S. L., Li, M., de Jong, W., and Kortlever, R. (2023). "Tuning the properties of N-doped biochar for selective CO₂ electroreduction to CO," *ACS Catal.* 13(15), 10309-10323. DOI: 10.1021/acscatal.3c01773
- Han, N., Ding, P., He, L., Li, Y., and Li, Y. (2019). "Promises of main group metal—based nanostructured materials for electrochemical CO₂ reduction to formate," *Adv. Energy Mater.* 10(11), article 1902338. DOI: 10.1002/aenm.201902338
- Hu, X., Yang, H., Guo, M., Gao, M., Zhang, E., Tian, H., Liang, Z., and Liu, X. (2018). "Synthesis and characterization of (Cu, S) Co-doped SnO₂ for electrocatalytic reduction of CO₂ to formate at low overpotential," *ChemElectroChem.* 5(9), 1330-1335. DOI: 10.1002/celc.201800104
- Hu, K., Jia, S. N., Shen, B. X., Wang, Z. Q., Dong, Z. J., and Lyu, H. H. (2024). "Nickel phthalocyanine anchored onto N-doped biochar for efficient electrocatalytic carbon dioxide reduction," *CHEM ENG J.* 497, article 154686. DOI: 10.1016/j.cej.2024.154686

- Jeong, S., Ohto, T., Nishiuchi, T., Nagata, K., Fujita, J. I., and Ito, Y. (2021).
 "Polyethylene glycol covered Sn catalysts accelerate the formation rate of formate by carbon dioxide reduction," ACS Catal. 11, 9962-9969. DOI:
 10.1021/acscatal.1c02646
- Jiang, L. H., Sun, G. Q., Zhou, Z. H., Sun, S. G., Wang, Q., Yan, S. Y., Li, H. Q., Tian, J., Guo, J. S., Zhou, B., and Xin, Q. (2005). "Size-controllable synthesis of monodispersed SnO₂ nanoparticles and application in electrocatalysts," *J. Phys. Chem. B.* 109, 8774-8778. DOI: 10.1021/jp050334g
- Jouny, M., Luc, W., and Jiao, F. (2018). "General techno-economic analysis of CO₂ electrolysis systems," *Ind. Eng. Chem. Res.* 57(6), 2165-2177. DOI: 10.1021/acs.iecr.0c01513
- Kim, Y. E., Lee, W., Youn, M. H., Jeong, S. K., Kim, H. J., Park, J. C., and Park, K. T. (2019). "Leaching-resistant SnO₂/γ-Al₂O₃ nano catalyst for stable electrochemical CO₂ reduction into formate," *Ind Eng Chem Res.* 78, 73-78. DOI: 10.1016/j.jiec.2019.05.042
- Lin, C., Xu, Z. F., Kong, X. D., Zheng, H., Geng, Z. G., and Zeng, J. (2022). "Lysine functionalized SnO₂ for efficient CO₂ electroreduction into formate," *ChemNanomMat.* 18, article e202200020. DOI: 10.1002/cnma.202200020
- Liu, Y. Y., Fan, M. Y., Zhang, X., Zhang, Q., Guay, D., and Qiao, J. L. (2017). "Design and engineering of urchin-like nanostructured SnO₂ catalysts via controlled facial hydrothermal synthesis for efficient electro-reduction of CO₂," *Electrochim. Acta*. 248, 123-132. DOI: 10.1016/j.electacta.2017.07.140
- Lu, L., Sun, X., Ma, J., Zhu, Q., Wu, C., Yang, D., and Han, B. (2017). "Selective electroreduction of carbon dioxide to formic acid on electrodeposited SnO₂@N-doped porous carbon catalysts," *Sci. China Chem.* 61(2), 228-235. DOI: 10.1007/s11426-017-9118-6
- Meng, N., Liu, C., Liu, Y., Yu, Y., and Zhang, B. (2019b). "Efficient electrosynthesis of syngas with tunable CO/H₂ ratios over ZnxCd1-xS-amine inorganic-organic hybrids," *Angew. Chem. Int. Edit.* 58, 18908-18912. DOI: 10.1002/anie.201913003
- Meng, Y., Jiang, J., Aihemaiti, A., Ju, T., Gao, Y., Liu, J., and Han, S. (2019a). "Feasibility of CO₂ capture from O₂-containing flue gas using a poly(ethylenimine)-functionalized sorbent: Oxidative stability in long-term operation," *ACS Appl. Mater. Interfaces* 11, 33781-33791. DOI: 10.1021/acsami.9b08048
- Mulik, B. B., Bankar, B. D., Munde, A. V., Chavan, P. P., Biradar, A. V., and Sathe, B. R. (2021). "Electrocatalytic and catalytic CO₂ hydrogenation on ZnO/g-C₃N₄ hybrid nanoelectrodes," *Appl. Surf. Sci.* 538, article 148120. DOI: 10.1016/j.apsusc.2020.148120
- Petrovic, B., Gorbounov, M., and Soltani, S. M. (2021). "Influence of surface modification on selective CO₂ adsorption: A technical review on mechanisms and methods," *Micropor. Mesopor. Mat.* 312, article 110751. DOI: 10.1016/j.micromeso.2020.110751
- Sun, Z., Fischer, J. M. T. A., Li, Q., Hu, J., Tang, Q., Wang, H., Wu, Z., Hankel, M., Searles, D. J., and Wang, L. (2017). "Enhanced CO₂ photocatalytic reduction on alkali-decorated graphitic carbon nitride," *Appl. Catal. B-Environ.* 216, 146-155. DOI: 10.1016/j.apcatb.2017.05.064
- Tan, Y. C., Jia, S., Tan, J., Leow, Y., Zheng, R., Tan, X. Y., Dolmanan, S. B., Zhang, M., Yew, P. Y. M., and Ni, X. P. (2023). "Coconut husk-derived biochar for enhancing electrochemical conversion of CO₂," *Mater. Today Chem.* 30, article 101595. DOI:

- 10.1016/j.mtchem.2023.101595
- Tay, Y. F., Tan, Z. H., and Lum, Y. W. (2021). "Engineering Sn-based catalytic materials for efficient electrochemical CO₂ reduction to formate," *ChemNanoMat.* 7, 380-391. DOI: 10.1002/cnma.202100031
- Tian, Y. H., Li, M., Wu, Z. Z., Sun, Q., Yuan, D., Johannessen, B., Xu, L., Wang, Y., Dou, Y. H., Zhao, H. J., and Zhang, S. Q. (2022). "Edge-hosted atomic Co-N₄ sites on hierarchical porous carbon for highly selective two-electron oxygen reduction reaction," *Angew. Chem. Int. Edit.* 61. DOI: 10.1002/anie.202213296.
- Wang, G., Chen, J., Li, K., Huang, J., Huang, Y., Liu, Y., Hu, X., Zhao, B., Yi, L., Jones, T. W., and Wen, Z. (2022). "Cost-effective and durable electrocatalysts for Coelectrolysis of CO₂ conversion and glycerol upgrading," *Nano Energy*. 92, 106751-106760. DOI: 10.1016/j.nanoen.2021.106751
- Yua, J. L., Liu, H. Y., Song, S. Q., Wang, Y., and Tsiakaras, P. (2017). "Electrochemical reduction of carbon dioxide at nanostructured SnO₂/carbon aerogels: The effect of tin oxide content on the catalytic activity and formate selectivity," *Appl Catal A-Gen*. 545, 159-166. DOI: 10.1016/j.apcata.2017.07.043
- Yuan, Y. S., Sheng, K., Zhuang, G. L., Li, Q. Y., Dou, C., Fang, Q. J., Zhan, W. W., Gao, H., Sun, D., and Han, X. G. (2021). "Collaboratively boosting charge transfer and CO₂ chemisorption of SnO₂ to selectively reduce CO₂ to HCOOH," *ChemCommun*. 57, 8636-8639. DOI: 10.1039/d1cc01818c
- Yu, J. L., Liu, H. Y., Song, S. Q., Wang, Y., and Tsiakaras, P. (2017). "Electrochemical reduction of carbon dioxide at nanostructured SnO₂/carbon aerogels: The effect of tin oxide content on the catalytic activity and formate selectivity," *Appl. Catal.*, A. 545, 159-166. DOI: 10.1016/j.apcata.2017.07.043
- Yue, Y., Zou, X. H., Shi, Y. D., Cai, J. N., Xiang, Y. X., Li, Z. S., and Lin, S. (2023). "A low crystallinity CuO-SnO₂/C catalyst for efficient electrocatalytic reduction of CO₂," *J Electroanal Chem.* 928, article 117089. DOI: 10.1016/j.jelechem.2022.117089
- Zhang, S., Kang, P., and J. Meyer, T. (2014). "Nanostructured tin catalysts for selective electrochemical reduction of carbon dioxide to formate," *J. Am. Chem. Soc.* 136, 1734-1737. DOI: 10.1021/ja4113885
- Zhang, B., Chen, S., Wulan, B., and Zhang, J. (2021). "Surface modification of SnO₂ nanosheets via ultrathin N-doped carbon layers for improving CO₂ electrocatalytic reduction," *Chem Eng J.* 421, article 130003. DOI: 10.1016/j.cej.2021.130003
- Zhang, B., Song, D. Z., Liu, Y. Z., Deng, Q. X., Yuan, Y., Liu, Q. Q., and Huo, J. (2023). "Porosity engineering of biochar-based single-atom Ni catalysts to promote CO₂ electroreduction over a broad potential window," *AICHE J.* 69, 18175. DOI: 10.1002/aic.18175

Article submitted: August 6, 2024; Peer review completed: September 7, 2024; Revised version received: September 19, 2024; Accepted: September 22, 2024; Published: October 10, 2024.

DOI: 10.15376/biores.19.4.9049-9059